

PCCP

Accepted Manuscript



This is an *Accepted Manuscript*, which has been through the Royal Society of Chemistry peer review process and has been accepted for publication.

Accepted Manuscripts are published online shortly after acceptance, before technical editing, formatting and proof reading. Using this free service, authors can make their results available to the community, in citable form, before we publish the edited article. We will replace this *Accepted Manuscript* with the edited and formatted *Advance Article* as soon as it is available.

You can find more information about *Accepted Manuscripts* in the [Information for Authors](#).

Please note that technical editing may introduce minor changes to the text and/or graphics, which may alter content. The journal's standard [Terms & Conditions](#) and the [Ethical guidelines](#) still apply. In no event shall the Royal Society of Chemistry be held responsible for any errors or omissions in this *Accepted Manuscript* or any consequences arising from the use of any information it contains.

H/D exchange in reactions of OH⁻ with D₂ and of OD⁻ with H₂ at low temperatures

Dmytro Mulin,^a Štěpán Roučka,^{*a} Pavol Jusko,^a Illia Zymak,^a Radek Plašil,^a Dieter Gerlich,^b Roland Wester,^c and Juraj Glosík^a

Received Xth XXXXXXXXXXXX 20XX, Accepted Xth XXXXXXXXXXXX 20XX

First published on the web Xth XXXXXXXXXXXX 200X

DOI: 10.1039/b000000x

Using a cryogenic linear 22-pole rf ion trap, rate coefficients for H/D exchange reactions of OH⁻ with D₂ (1) and OD⁻ with H₂ (2) have been measured at temperatures between 11 K and 300 K with normal hydrogen. Below 60 K, we obtained $k_1 = 5.5 \times 10^{-10} \text{ cm}^3 \text{ s}^{-1}$ for the exoergic reaction (1). Increasing the temperature above 60 K, the data decrease with a power law, $k_1(T) \sim T^{-2.7}$, reaching $\approx 1 \times 10^{-10} \text{ cm}^3 \text{ s}^{-1}$ at 200 K. This observation is tentatively explained with a decrease of the lifetime of the intermediate complex as well as with the assumption that scrambling of the three hydrogen atoms is restricted by the topology of the potential energy surface. The rate coefficient for the endoergic reaction (2) increases with temperature from 12 K up to 300 K, following the Arrhenius equation, $k_2 = 7.5 \times 10^{-11} \exp(-92 \text{ K}/T) \text{ cm}^3 \text{ s}^{-1}$ over two orders of magnitude. The fitted activation energy, $E_{\text{A-Exp}} = 7.9 \text{ meV}$, is in perfect accordance with the endothermicity of 24.0 meV, if one accounts for the thermal population of the rotational states of both reactants. The low mean activation energy in comparison with the enthalpy change in the reaction is mainly due to the rotational energy of 14.7 meV contributed by ortho-H₂($J = 1$). Nonetheless, one should not ignore the reactivity of pure para-H₂ because, according to our model, it already reaches 43 % of that of ortho-H₂ at 100 K.

1 Introduction

Interactions of ions with neutral particles and the formation of new molecules play important roles in natural and technical plasmas. The various ways to form interstellar molecules, including gas phase processes involving cations, radicals and gas-grain interactions have attracted a lot of attention in the last four decades. The role of anions in the interstellar medium has been discussed for the first time by Dalgarno and McCray already in 1973¹. However, the interest in anions diminished because, due to a lack of spectroscopic data, they could not be detected. This has changed recently when the first anions were observed in the interstellar medium²⁻⁴, reactivating the interest in theory^{5,6} and experiments⁷⁻¹³ with anion-molecule reactions, including associative detachment reactions. Also photodetachment of electrons from anions including interstellar anions has been reported¹⁴⁻¹⁷. The anions are interesting not only due to their role in astrochemistry, but they also play an important role in plasma physics, in technical discharges, in radiation chemistry etc.¹⁸⁻²⁰.

Experimental and theoretical studies of gas phase reactions provide a good basis for understanding the detailed dynamics of fundamental chemical reactions. Here, reactions of hydrogen atoms or molecules are of particular importance, because at low temperature, the influence of specific molecular quantum states can be probed^{9-11,21-23}. Furthermore, theoretical treatments of reactive scattering process, while still challenging, becomes feasible for few-atom systems^{24,25}. A particular class of reactions is the hydrogen/deuterium isotopic exchange²⁶, which forms products that are chemically equivalent to the reactants and whose energies vary only by their change in vibrational zero-point energy.

We recently studied H/D isotope effects in the reactions H⁻(D⁻) + H and O⁻ + H₂ (D₂) using the AB-22-pole ion trap apparatus^{10,27,28} and we measured the temperature dependencies of their reaction rate coefficients for temperatures from 11 K up to 300 K. In the present study we investigate the H/D exchange process at low temperature in a more complex collision system, OH⁻ + H₂ and its isotopic variants, where isotopic exchange occurs via the H₃O⁻ complex and requires several chemical rearrangement steps. As such, this system is different from H/D exchange in many cation-molecule reactions²⁶.

The first experimental observation of the long-lived H₃O⁻ anion has been reported in 1983 by Kleingeld and Nibbering²⁹. One of the formation mechanisms is ternary associa-

^a Department of Surface and Plasma Science, Faculty of Mathematics and Physics, Charles University in Prague, Czech Republic Tel: +420 22191 2344; E-mail: Stepan.Roucka@mff.cuni.cz

^b Department of Physics, Technische Universität Chemnitz, Germany

^c Institute for Ion Physics and Applied Physics, University of Innsbruck, Austria

tion of $\text{OH}^- + \text{H}_2$, with He or H_2 as third body. A ternary rate coefficient of $10^{-30} \text{ cm}^6 \text{ s}^{-1}$ was measured at 88 K³⁰, which increases for $\text{OD}^- + \text{D}_2$ to $3 \times 10^{-29} \text{ cm}^6 \text{ s}^{-1}$ at 15 K³¹. The stability of this anion made it possible to probe the transition state of $\text{OH} + \text{H}_2 \rightarrow \text{H}_2\text{O} + \text{H}$ by starting the neutral reaction via photodetachment from the anion^{32–34}. These very interesting experiments stimulated state of the art calculations including accurate potential energy surfaces of H_3O^- and the neutral H_3O complex^{32,33}.

The endothermic proton transfer reaction $\text{OH}^- + \text{H}_2 \rightarrow \text{H}^- + \text{H}_2\text{O}$ proceeds via the H_3O^- collision complex. The enthalpy change in this reaction is in the range $\Delta H = 0.37 \text{ eV} - 0.46 \text{ eV}$, the uncertainty of ΔH reflects values given in previous publications^{30,32,33,35,36}. Collisions of H^- with H_2O were studied in the first anion-molecule experiment³⁷. Crossed molecular beam experiments indicated that the reaction proceeds via a direct mechanism at collision energies above 0.7 eV³⁸. In a 4 K 22-pole ion trap, this reaction could be promoted by exciting the first vibrational state of the anion with 2.85 μm IR radiation³⁶.

A common way to probe reaction dynamics and to learn more about the H_3O^- collision complex is to use isotope labelling and to look for scrambling of the chemically equivalent atoms. In the following, we will discuss the two isotope exchange reactions, which have been studied experimentally before^{38–42},



The majority of previous studies of these reactions were carried out at 300 K and above^{39,41,43}. There is just one flow drift tube study at 130 K and there are no data available for lower temperatures⁴⁰.

The reaction enthalpies at 0 K given in Eq. (1) and (2) were calculated from electron affinities of OH and OD^{44,45}, zero point energies of H_2 , D_2 , and HD⁴⁶, and from zero point energies of OH and OD^{47,48} in the Born-Oppenheimer approximation. However, at sub-meV accuracy, the isotopic electronic shifts of the energy eigenvalues need to be accounted for. It has been shown for several isotope exchange reactions with H_2 and D_2 that the change of enthalpy due to adiabatic correction of the Born-Oppenheimer approximation is on the order of 1 meV^{49–51}. In particular, spectroscopic studies of OH and OD suggest that the isotopic shift of electronic ground state potential energy surface in this system can be up to 2.5 meV (see note 78 in Ruscic *et al.*⁵²). To our knowledge, there are no published results concerning the OH/OD isotopic shift, so in the worst case, the error of the above determined endothermicities can be up to 2.5 meV.

For better understanding of the collision complex, Fig. 1 provides a sketch of the stationary points of different isotopic

and isomeric configurations of the H_2DO^- system involved in reaction (2). It has been already discussed^{39,40} that, for H/D exchange, the system has to pass through three minima, separated by submerged transition states (TS). The energies shown in Fig. 1 are corrected for zero point energies. As already mentioned above, the endothermicity of 24.0 meV is known with good precision. The values for the deuterated intermediates are estimated from H_3O^- energies calculated by Zhang *et al.*³³ corrected for the rather uncertain zero point energies reported by Wang *et al.*³⁵. Inspection reveals that, during the approach of the reactants, first an $\text{OH}^- \cdot (\text{H}_2)$ complex is formed, which can undergo rearrangement to the most stable form of H_3O^- , an H^- ion bound to a perturbed H_2O molecule. With exception of the zero point energies, the exit channel is symmetric. It is not so easy to predict, where scrambling of H and D atoms actually occurs, most probably in the transition states where both the H_2 bond and one of the HO bonds is weakened. Extending this picture to all dimensions one may expect that the outcome of complex formation in the first minimum, isotope exchange around the minimum, and break-up either back to reactants or to products may be predictable with a statistical model. However, the submerged barriers, centrifugal barriers, and the rather rigid structures in the potential minima may hinder full scrambling. In total the probability for H/D exchange may depend on the relative orientation of the reactants during the approach, on the initial rotational states of both reactants, on the relative velocity, and certainly also on the total orbital angular momentum of the collision complex.

To compare quantitatively rotational excitation of both reactants with the endothermicity of reaction (2), we included in the left panel of Fig. 1 the energies of two lowest rotational states of H_2 with para ($J_{\text{H}_2} = 0$) and ortho ($J_{\text{H}_2} = 1$) nuclear spin configuration as well as the four lowest rotational states of the OD^- ion⁵³.

2 Experimental

The experiments have been carried out using the AB-22PT instrument^{54,55}. The principle of operating a 22-pole ion trap has been described many times so only a few essential details will be given here. For detailed descriptions, discussions of specific features, and comparisons between 22-pole trap experiments see references^{10,54,56–61}.

The 22-pole trap was operated at an RF frequency of 27 MHz, the amplitude has been set to values up to 40 V (peak to peak). The temperature has been varied from 11 K to 300 K. The instrument uses ultra-high vacuum technology, the background number density of residual gas in the trap volume was at most 10^8 cm^{-3} at 11 K. High purity H_2 or D_2 gases were used in the experiments as reactants and He as buffer gas. Hydrogen or deuterium was used in its “normal” composition,

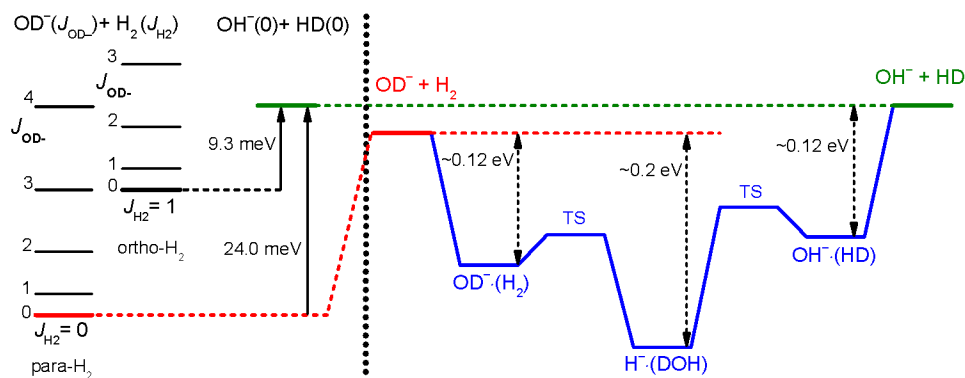


Fig. 1 Right panel: Stationary points of the potential energy surface for the reaction $\text{OD}^- + \text{H}_2 \longrightarrow \text{OH}^- + \text{HD}$. The energies are corrected for zero point energies, for details, see text. The arrows (with dashed lines) indicate the binding energies of the intermediate complexes $\text{OD}^- \cdot (\text{H}_2)$, $\text{OH}^- \cdot (\text{HD})$ and $\text{H}^- \cdot (\text{DOH})$. Left panel: Rotational energy levels^{47,53} of OD^- and H_2 . The two arrows indicate the energies required for forming ground state products.

i.e., with a ortho : para ratio of 3 : 1 or 2 : 1, respectively. Tests have indicated that this population does not change while passing the gas into the cooled trap via the inlet system^{62,63}.

OH^- or OD^- ions are produced in the electron impact storage ion source using a mixture of N_2O and H_2 or D_2 ^{27,28}. The desired ions are then selected by a quadrupole mass filter and guided into the trap, where they are stored. A He/D_2 or a He/H_2 gas mixture is introduced directly into the trap volume. After various well-defined trapping times the trap is opened, the ions are mass selected by the second quadrupole mass spectrometer, and finally counted using an MCP detector. The actual reactant density is adjusted so that the decay of the number of trapped reactant ions due to the reaction is statistically significant. For the fast exothermic reaction (1), the D_2 number density was varied between 10^{10} cm^{-3} and 10^{12} cm^{-3} while for the slow endoergic reaction (2) the H_2 number density has been increased up to 10^{13} cm^{-3} .

Helium buffer gas was added to the trap volume to cool the reactant ions. The actual density of He was such that reactant ions would have at least 10 collisions with He prior to collision with a molecule of reactant gas. This ensures that the kinetic and internal temperatures of OH^- or OD^- ions are thermalized at temperature of the He buffer gas prior to reaction.

The temperature of trapped ions thermalized by the buffer gas was studied and discussed in many experimental studies. It was found that trap imperfections or patch potentials may lead to acceleration of the ions (i.e., higher kinetic energies). It was concluded several times for the present trap that the interaction temperature is close to the trap temperature (see e.g. refs^{57,63}). In some previous studies the ion temperature was obtained by measuring the temperature dependence of reaction rate coefficients where this dependence could be extrapolated, e.g. rate of the ternary association reaction of $\text{He}^+ + \text{He} + \text{He}$ ⁵⁷. In the present experiments, the reaction of OD^- with H_2 is endothermic

and has an Arrhenius-type temperature dependence of the reaction rate coefficient. Relying on the endothermicity allows us to estimate that the collision temperature deviates from the trap temperature $T_{22\text{PT}}$ by less than 5 K.

In the experimental studies of reactions (1) or (2), a small amount of H_2 or D_2 , respectively, always leaks into the trap from the ion source, and the product ions react with these gases via reactions (2) or (1), respectively. In this way products are reconverted back to reactant ions. Note that these reactions are not the reverse reactions of (1) or (2), the presence of HD is negligible. Although the number density of gas from the ion source is very small compared to the reactant number density (see Table 1), it is necessary to include its influence in the data analysis, especially for the endothermic reaction (2). Consequently, the reaction rate coefficients for reactions (1) and (2) are determined by fitting the time dependence of the measured number of ions with the solution of the balance equations

$$\frac{d}{dt}N_{\text{OH}^-} = -k_1N_{\text{OH}^-}[\text{D}_2] + k_2N_{\text{OD}^-}[\text{H}_2] \quad (3)$$

$$\frac{d}{dt}N_{\text{OD}^-} = k_1N_{\text{OH}^-}[\text{D}_2] - k_2N_{\text{OD}^-}[\text{H}_2] \quad (4)$$

where k_1 and k_2 are the binary reaction rate coefficients of the reaction (1) and (2), respectively. $[\text{H}_2]$ and $[\text{D}_2]$ are hydrogen and deuterium number densities in the trap, respectively. N_{OH^-} and N_{OD^-} are numbers of detected OH^- and OD^- ions, respectively. The free parameters of the fit were the reaction rates $r_1 = k_1[\text{D}_2]$ and $r_2 = k_2[\text{H}_2]$ as well as the initial numbers of trapped ions.

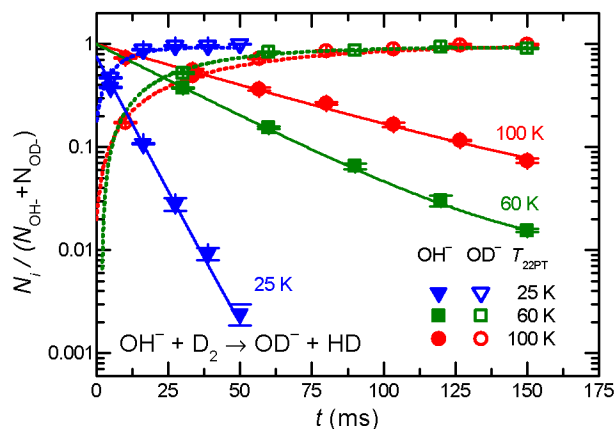


Fig. 2 Normalized number of primary ions (OH^- , closed symbols) and product ions (OD^- , open symbols) as a function of storage time. Operating conditions were $T_{22\text{PT}} = 25, 60, 100$ K, the densities of D_2 , He, and H_2 are listed in Table 1.

Table 1 Experimental conditions used for the results shown in Fig. 2. Lower index SIS indicates the density of hydrogen penetrating into the trap from the Storage Ion Source (SIS).

$T_{22\text{PT}}$	$[\text{D}_2]$ (cm^{-3})	$[\text{He}]$ (cm^{-3})	$[\text{H}_2]_{\text{SIS}}$ (cm^{-3})
25 K	2.1×10^{11}	6.0×10^{12}	$\approx 6 \times 10^9$
60 K	6.0×10^{10}	2.4×10^{12}	$\approx 3 \times 10^9$
100 K	4.7×10^{10}	4.1×10^{12}	$\approx 1 \times 10^9$

3 Results and Discussion

3.1 Reaction $\text{OH}^- + \text{D}_2$

As a typical result, Fig. 2 shows the decline of primary ions, N_{OH^-} , and the increase of products, N_{OD^-} , at three temperatures. For normalizing, the numbers of ions are divided by the sum $N_{\text{OH}^-} + N_{\text{OD}^-}$. This sum did not change with time indicating that there is no loss of ions or that there are no other products. The experimental conditions for these results are summarized in Table 1. Note that the number density of He buffer gas is at least 10 times higher than that of the reactant gas D_2 . The density of the perturbing H_2 gas, originating from the ion source, is more than 10 times lower. The monoexponential decay of the primary ions in Fig. 2 indicates that reconversion of products can be neglected in the case of the exothermic reaction (1). The binary character of reaction (1) was checked by varying the number density $[\text{D}_2]$ from $2 \times 10^9 \text{ cm}^{-3}$ up to $4 \times 10^{11} \text{ cm}^{-3}$. The data plotted in Fig. 3 for 3 temperatures confirm the linear relationship $r_1 = k_1 [\text{D}_2]$.

The measured temperature dependence of the rate coefficient k_1 for reaction (1) is shown in Fig. 4. As already men-

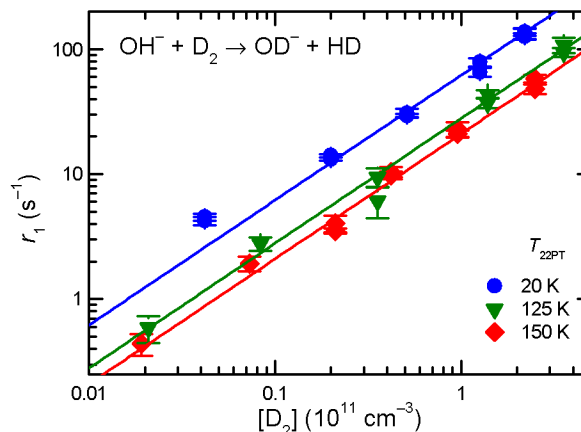


Fig. 3 Rate r_1 of the reaction (1) as a function of deuterium number density $[\text{D}_2]$ at trap temperatures $T_{22\text{PT}} = 20, 125, 150$ K.

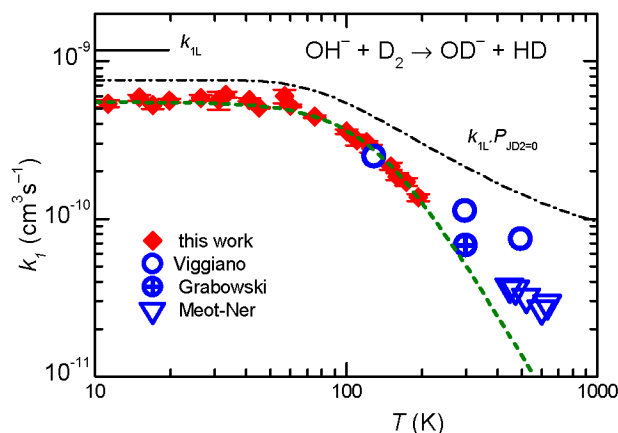


Fig. 4 Measured temperature dependence of the rate coefficient k_1 for H/D exchange reaction (1). The calculated Langevin collisional rate coefficient is indicated as k_{IL} . The assumption that exclusively the rotational ground state of D_2 can react leads to the dash-dotted line (see text). Thermal FDT data of Viggiano and Morris⁴⁰, SIFT data of Grabowski *et al.*³⁹, and HPMS data of Mautner *et al.*⁴¹ are also included. The dashed line shows $k_1(T)$ calculated from equation (5) with the parameters given there.

tioned, normal D_2 is used as the reactant. For comparison, the Langevin collisional rate coefficient k_{1L} for $OH^- + D_2$ capture is indicated. The measurements were conducted in the range of trap temperatures T_{22PT} from 11 K up to 200 K. The data show that above 60 K the reaction is getting slower with increasing temperature. The previous thermal data from selected ion flow tube (SIFT) of Grabowski *et al.*³⁹ and flow drift tube (FDT) obtained by Viggiano and Morris⁴⁰ are included in the graph. High temperature data obtained in high pressure mass spectrometer experiment (HPMS) are also plotted⁴¹. We did not include FDT data at elevated collisional energy (KE_{CM}) because of unclear internal excitation of the ions⁴⁰. In their FDT study, Viggiano and Morris⁴⁰ measured k_1 both as a function of the D_2 temperature and of KE_{CM} (kinetic energy in the center of mass for collision between D_2 and OH^- ions). They observed a significant negative dependence on the temperature but only a slight dependence on the kinetic energy. Therefore they concluded that the negative temperature dependence must be due to the increasing rotational temperature of D_2 . To illustrate the influence of the rotational population of deuterium in our temperature range, Fig. 4 shows a simple model rate coefficient (dash-dotted line), calculated with the assumptions that only the rotational ground state can react and this with the Langevin rate coefficient k_{1L} . At first sight there seems to be a similarity in the temperature dependence of this function with the measured data; however, the decline of our experimental data is much steeper. In our temperature range, it must be due to the increase of the energy contributed from all degrees of freedom. This leads to a decrease of the life time of the collision complex in the first minimum (see Fig. 1). In this context we note that the comparison of k_{1L} with the data measured below 60 K also leads to the supposition that, even at these low energies, many collision complexes decay back to reactants rather quickly. To get more insight into the detailed dynamics of this reaction, more detailed experiments as well as theoretical studies are needed.

Negative temperature dependences have been observed for many binary reactions proceeding via formation of intermediate complex. For such reactions it was deduced that the temperature dependence of the rate coefficient can be approximated by a power law dependence^{64–70} in analogy with the mechanism of ternary reactions described by Bates⁷¹ and Herbst⁷².

To describe the studied reaction (1), we are going to use a semi-empirical method given e.g. by Glosik *et al.*⁷⁰. The general conclusion of this semi-empirical description is that the reaction rate coefficient k_1 can be described by the dependence:

$$\frac{k_{10}}{k_1} - 1 = \left(\frac{T}{T_0}\right)^m \quad (5)$$

with parameters k_{10} , T_0 and m . From the fit plotted in Fig. 4 we obtained the parameters $k_{10} = 5.5 \times 10^{-10} \text{ cm}^3 \text{ s}^{-1}$, $T_0 =$

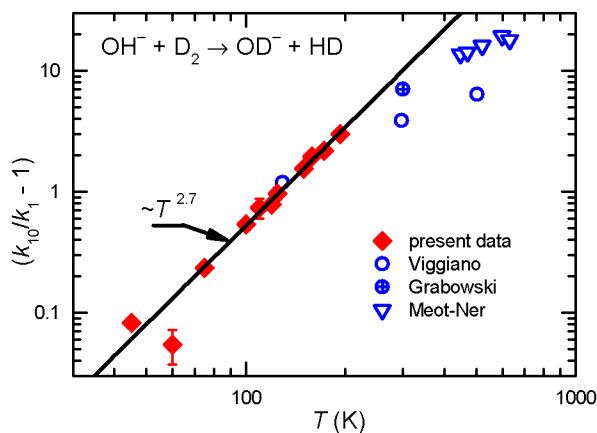


Fig. 5 Plot of $(k_{10}/k_1 - 1)$ versus T for the data shown in Fig. 4 emphasizing on the power law T^m . Data with a statistical error above 100% in this representation are not shown.

130 K, and $m = 2.7 \pm 0.5$. The error estimate of m includes the statistical error as well as the error due to possible deviations from the power law, which was estimated by fitting subsets of data in different temperature ranges. The validity of equation (5) for describing the measured data can be more easily seen from the plot of $\log(k_{10}/k_1 - 1)$ versus $\log(T)$, shown in Fig. 5. This plot includes also data from FDT⁴⁰, HPMS⁴¹ and SIFT³⁹.

The empirical model leading to equation (5) also can be derived from RRKM theory and the exponent m can be explained with the number of “active” degrees of freedom of both the reactants and of the intermediate complex. However, looking at Fig. 1, it is not obvious, where the rate limiting bottlenecks really are. In any case, the fit through the data plotted in Fig. 4 and the linearity of the plot in Fig. 5 may be significant. The extrapolation of our fit towards higher temperatures gives a reasonable prediction for previous data, see Figs. 4 and 5. The discrepancy between the empirical curve and the data of Mautner *et al.*⁴¹ at higher temperatures must be due to direct mechanisms, which is not accounted for in equation (5). Similar behavior has been observed before for several ion molecule reactions⁶⁵. The significant contribution of the present study is the coverage of a large interval at low temperatures.

3.2 Reaction $OD^- + H_2$

Examples of the measured time evolutions of normalized numbers of primary OD^- and product OH^- ions at four different temperatures are plotted in Fig. 6. The actual densities of H_2 , He and D_2 in the trap are listed in Table 2. High number densities of H_2 are necessary to obtain a significant decay of the number of primary OD^- anions because at low

Table 2 Experimental conditions used for the results shown in Fig. 6. $[D_2]_{SIS}$ is the density of deuterium penetrating from the storage ion source into the trap.

T_{22PT}	$[H_2]$ (cm^{-3})	$[He]$ (cm^{-3})	$[D_2]_{SIS}$ (cm^{-3})
12 K	1.2×10^{13}	3.4×10^{13}	$\approx 1 \times 10^{10}$
21 K	6.7×10^{12}	4.5×10^{13}	$\approx 1 \times 10^{10}$
78 K	2.0×10^{12}	2.3×10^{13}	$\approx 5 \times 10^9$
200 K	3.4×10^{11}	2.5×10^{12}	$\approx 3 \times 10^9$

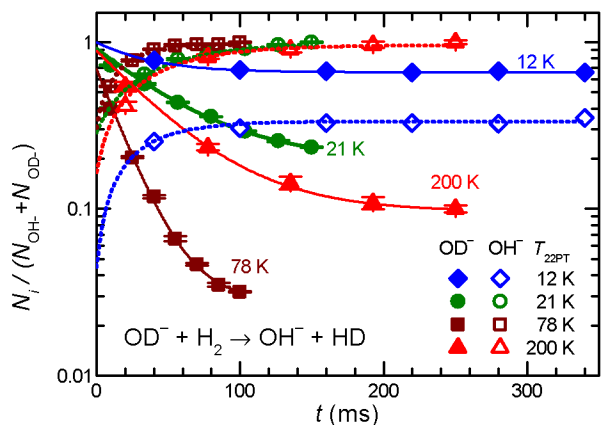


Fig. 6 Normalized number of primary ions (OD^- , closed symbols) and product ions (OH^- , open symbols) as a function of storage time. The trap was at $T_{22PT} = 12, 21, 78, 200$ K, the densities of D_2 , He and H_2 in the trap are listed in Table 2.

temperatures the endothermic reaction (2) is slow. Note that, in comparison with the density of reactant H_2 , the density of D_2 from the SIS is at least 100 times lower. In spite of this, back conversion of the OH^- products via exothermic H/D exchange with D_2 dominates at low temperatures. Therefore, the influence of reconversion cannot be neglected. Non-monoexponential decay is a clear indication of this fact. From this we can observe an approach towards equilibrium already at $t > 50$ ms at 12 K (see Fig. 6). There reconversion is the factor limiting the accuracy of k_2 .

The temperature dependence of reaction (2) was studied in the range of trap temperatures T_{22PT} from 11 K to 300 K. Varying the target density, it was confirmed that the products are formed via a bimolecular reaction. Our data shown in Fig. 7 were fitted by the Arrhenius function $k_2 = k_{2A} \exp(-E_{A-Exp}/k_B T)$, where k_{2A} is pre-exponential factor and E_{A-Exp} is the Arrhenius activation energy⁷³. From the fit we obtained $k_{2A} = 7.5 \times 10^{-11} \text{ cm}^3 \text{ s}^{-1}$ and $E_{A-Exp} = (7.9 \pm 0.3) \text{ meV}$, corresponding to $T_{A-Exp} = E_{A-Exp}/k_B = (92 \pm 3) \text{ K}$. The obtained function agrees with the data obtained in previous FDT experiments of Viggiano and Morris⁴⁰ as well. To

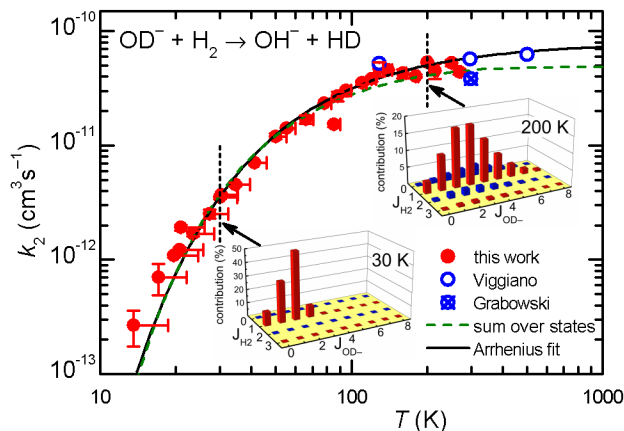


Fig. 7 Temperature dependence of the rate coefficient k_2 (filled circles) for the endothermic reaction (2). The vertical error bars of the two points at the lowest temperatures include the estimated error caused by the oscillations of temperature and pressure. At temperatures above 20 K, these effects are negligible and only statistical errors are shown. The results have been fitted using an Arrhenius temperature dependence (solid line). Previous FDT data of Viggiano and Morris⁴⁰ and SIFT data of Grabowski *et al.*³⁹ are also plotted. The dashed curve is a fit with function (7) (see the text for details). The insets indicate the $k_{J_{H_2}J_{OD^-}}/k_{2\Sigma}$ in percent (Eq. 6 and 7) at 30 K and 200 K.

emphasize the low temperature region, Fig. 8 shows the data as Arrhenius plot, revealing a linear decay over two orders of magnitude. Minor deviations are only at $T_{22PT} < 25$ K.

For explaining the difference between the endothermicity of reaction (2), $\Delta H = 24.0 \text{ meV}$, and the obtained activation energy $E_{A-Exp} = (7.9 \pm 0.3) \text{ meV}$, one is tempted to account simply for the rotational energy contributed from the hydrogen target. We use normal hydrogen with 75% in the ortho nuclear spin state. This means that, even at very low temperatures, 3/4 of the H_2 molecules are rotationally excited with odd quantum numbers. If the rotational energy for $J = 1$, 14.7 meV, is available for promoting the reaction, the threshold onset is already lowered to 9.3 meV. For a more consistent comparison, one has to account for all rotational energies provided by both reactants (see Fig. 1). Introducing a state specific rate coefficient $k_{J_{H_2}J_{OD^-}}$ for each combination of rotational states, J_{H_2} , J_{OD^-} and accounting for their thermal populations $P_{J_{H_2}}$ and $P_{J_{OD^-}}$, the thermal rate coefficient can be calculated using the sum

$$k_{2\Sigma}(T) = \sum_{J_{OD^-}, J_{H_2}} P_{J_{H_2}} P_{J_{OD^-}} k_{J_{H_2}J_{OD^-}} \quad (6)$$

This general formula can account for all dependencies, e.g. rotational inhibition or special nuclear spin effects. In the following we use the crude assumptions that all energies are

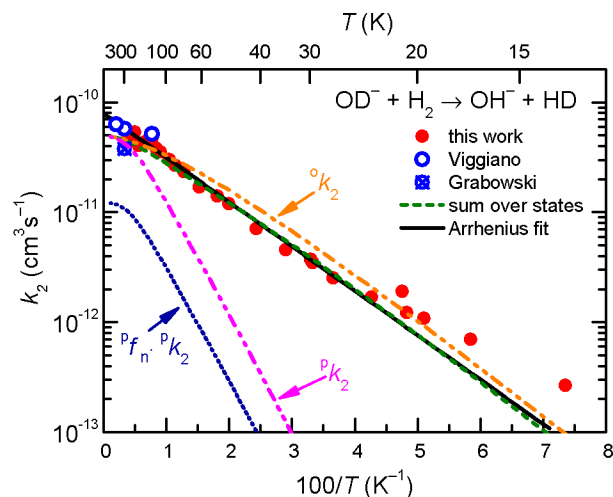


Fig. 8 Arrhenius plot of rate coefficient k_2 for reaction (2) measured with normal H_2 . Shown are two almost identical fits, the two-parameter Arrhenius (solid line) and the sum over all relevant rotational states of the ion and of normal hydrogen (no ortho-para relaxation, dashed line). For details see text. Previous FDT data of Viggiano and Morris⁴⁰ and SIFT data of Grabowski *et al.*³⁹ are also included in the plot. The plots marked with $^o k_2$ and $^p k_2$ are predictions for pure ortho- and para-hydrogen. In normal hydrogen, the contribution of para-hydrogen is only $^p f_n ^p k_2 = \frac{1}{4} ^p k_2$.

equivalent in driving the reaction and that we can use a global pre-exponential factor k_{20} in an Arrhenius representation for the state specific rate coefficients,

$$k_{J_{\text{H}_2} J_{\text{OD}^-}}(T) = k_{20} \exp\left(-\frac{\Delta E_{J_{\text{H}_2} J_{\text{OD}^-}}}{k_{\text{B}} T}\right). \quad (7)$$

The activation energy is given by

$$\Delta E_{J_{\text{H}_2} J_{\text{OD}^-}} = \max\{0; (\Delta H - E_{J_{\text{H}_2}} - E_{J_{\text{OD}^-}})\}. \quad (8)$$

The energies of the rotational states, $E_{J_{\text{H}_2}}$ and $E_{J_{\text{OD}^-}}$, have been calculated using the rotational constants from Huber and Herzberg⁴⁷, Rehffuss *et al.*⁵³. Using $\Delta H = 24.0$ meV as fixed and putting Eq. (7) into Eq. (6), the averaged rate coefficient $k_{2\Sigma}(T)$ is completely determined with the exception of one free parameter, k_{20} . Accounting for the temperature dependence of the rotational population of OD^- and the constant 1 : 3 population of even and odd J of normal H_2 , the experimental data could be fitted leading to $k_{20} = 4.9 \times 10^{-11} \text{ cm}^3 \text{ s}^{-1}$. Comparison of this result (dashed line) with the data points in Figs. 7 and 8 reveals good agreement over a wide range of T . The small deviations at low temperatures are most probably due to experimental uncertainties in the translational and rotational temperatures (they may differ slightly). It also cannot be excluded, that ΔH is slightly smaller. The problem of determining the endothermicity with sub-meV accuracy from the difference of zero point energies has been discussed above.

Based on our simple model, specific rate coefficients can be calculated for various conditions of the trapping experiment. The two insets in Fig. 7 show the relative contributions as a function of the two rotational states ($J_{\text{H}_2}, J_{\text{OD}^-}$). At 30 K, the largest rate coefficient is predicted for (1, 2) while at 200 K, also contributions from $J_{\text{H}_2} = 0$ and 2 show up. Summing exclusively over even or odd rotational states of H_2 leads to rate coefficients for pure ortho or pure para hydrogen, respectively. The results are shown in Fig. 8 as $^o k_2$ and $^p k_2$. The lowest curve in this plot, $^p f_n ^p k_2$, shows the contribution of para- H_2 in the present experiment, where normal- H_2 has been used ($^p f_n = 0.25$). Such predictions are important for preparing experiments with para-enriched H_2 or for estimating the product signal for a hydrogen beam, passing a trapped OD^- cloud.

4 Conclusion

We have studied the temperature dependence of proton-deuteron exchange for the two reactions (1) and (2). The experiments have been carried out using the AB-22PT instrument, the cold head of which can reach nominal temperatures as low as 10 K. Both the He buffer gas and the hydrogen reactant gas have been leaked into the trap directly resulting in a nearly thermalized system.

Isotope scrambling via the 0.2 eV bound intermediate H_3O^- is rather inefficient. This can be concluded from a comparison of the measured rate coefficients for the two isotopic combinations (1) and (2) with each other as well as with the corresponding capture values (Langevin: $k_{1\text{L}} = 1.16 \times 10^{-9} \text{ cm}^3 \text{ s}^{-1}$ and $k_{2\text{L}} = 1.55 \times 10^{-9} \text{ cm}^3 \text{ s}^{-1}$). Only at low temperatures, reaction (1) reaches almost 70% of $\frac{2}{3} k_{1\text{L}}$ (the pre-factor accounts for the 1 : 2 ratio of H : D). Reaction (2) is always slower than (1) and increases only to 5% of $\frac{2}{3} k_{2\text{L}}$. All this may indicate steric hindrance during complex formation or weak coupling between the various H_3O^- intermediates.

More information has been gained from the change of reactivity with increasing temperature. The measured negative temperature dependence of the exoergic reaction (1) has been approximated using the function $k_1 \approx k_{10}/(1 + (T/130 \text{ K})^{2.7})$. This power law and its similarity to the T dependence of three body association reactions leads to the supposition that a decrease of the complex lifetime may be responsible for the fall-off of the experimental data. A different explanation, proposed by Viggiano and Morris⁴⁰, postulates that rotation of D_2 hinders the reaction. This idea has been partly supported by Lee and Farrar⁴² who concluded that the reaction needs favorable alignments of OH^- and D_2 . This may be easier to reach with non-rotating deuterium. We have tested this idea by comparing our data with a simple simulation assuming that

exclusively $D_2(J=0)$ reacts. As can be seen from the dash-dotted line in Fig. 4, the resulting temperature dependence is not falling off steeply enough.

So far our results are not detailed enough for extracting state specific rate coefficients $k_{J_{H_2}J_{OD}}$; however, the results for the endoergic reaction (2) give additional hints. For modeling the increase of $k_2(T)$ we have assumed that each combination of rotational states of the two reactants contributes with the same rate coefficient multiplied with a state specific Arrhenius factor (see Eq. 7 and 8). The dashed line in Fig. 7 shows that this leads to a very good fit of our data with only one free parameter, k_{20} . It is also in accord with previous data^{39,40}.

In spite of our new results and their good agreement with the simple models, many questions remain open and ask for more experimental and theoretical activities. An obvious task is to use pure HD as target gas and to study reaction (1) and (2) in their reverse direction. The use of para-enriched hydrogen for separating $J=0$ and $J=1$ contributions already has been mentioned and work is in progress. For testing the dependence of k_1 on the rotation of the D_2 molecule, the AB-22PT instrument can be operated with a cold effusive D_2 beam instead of leaking the gas directly into the trap⁵⁴. The combination neutral beam - trap allows one to control the rotational population of the ions separately from that of the neutrals.

For a deeper understanding of the reaction dynamics, theoretical investigations are required. Potential energy surfaces are available^{33,34,38}. First hints to a possible orientation dependence during the approach of the reactants may be obtained from trajectory calculations. Trajectories, started somewhere in the three potential minima, may provide information on the efficiency of H/D scrambling. To look closer to the H_3O^- transition state, the spectroscopic characterization of this stable molecular anion is of great interest. Moreover, photofragmentation of the 0.2 eV bound H_3O^- may start selected half-collisions, complementary to the neutral reactions initiated by photo detachment of the electron from H_3O^- ³⁴.

Acknowledgements

The 22-pole ion trap instrument has been developed in Chemnitz and since 2009 it has been operated in the Faculty of Mathematics and Physics of the Charles University in Prague. We thank Chemnitz University of Technology and the DFG for making this transfer possible. This work was partly supported by GACR Grant No. P209/12/0233, 14-14715P, UNCE Grant No. 204020/2012, SV Grant No. 260 090, GAUK Grant No. 572214, 692214, 659112, AKTION 7AMB14AT023.

References

1 A. Dalgarno and R. A. McCray, *Astrophys. J.*, 1973, **181**, 95–100.

- 2 M. C. McCarthy, C. A. Gottlieb, H. Gupta and P. Thaddeus, *Astrophys. J.*, 2006, **652**, L141.
- 3 J. Cernicharo, M. Guélin, M. Agundez, K. Kawaguchi, M. McCarthy and P. Thaddeus, *Astron. & Astrophys.*, 2007, **467**, L37–L40.
- 4 S. Brunken, H. Gupta, C. A. Gottlieb, M. C. McCarthy and P. Thaddeus, *Astrophys. J.*, 2007, **664**, L43.
- 5 P. Botschwina and R. Oswald, *J. Phys. Chem. A*, 2010, **114**, 4875–4880.
- 6 Z. Yang, B. Eichelberger, O. Martinez, M. Stepanovic, T. P. Snow and V. M. Bierbaum, *J. Am. Chem. Soc.*, 2010, **132**, 5812–5819.
- 7 N. J. Demarais, Z. Yang, O. Martinez, N. Wehres, T. P. Snow and V. M. Bierbaum, *Astrophys. J.*, 2012, **746**, 32.
- 8 Z. Yang, B. Eichelberger, M. Y. Carpenter, O. Martinez, Jr., T. P. Snow and V. M. Bierbaum, *Astrophys. J.*, 2010, **723**, 1325–1330.
- 9 H. Kreckel, H. Bruhns, M. Čížek, S. C. O. Glover, K. A. Miller, X. Urbain and D. W. Savin, *Science*, 2010, **329**, 69–71.
- 10 D. Gerlich, P. Jusko, Š. Roučka, I. Zymak, R. Plašil and J. Glosík, *Astrophys. J.*, 2012, **749**, 22.
- 11 K. Miller, H. Bruhns, M. Čížek, J. Eliášek, R. Cabrera-Trujillo, H. Kreckel, A. O'Connor, X. Urbain and D. Savin, *Phys. Rev. A*, 2012, **86**, 032714.
- 12 C. A. Cole, N. J. Demarais, Z. Yang, T. P. Snow and V. M. Bierbaum, *Astrophys. J.*, 2013, **779**, 181.
- 13 E. S. Endres, O. Lakhmanskaya, D. Hauser, S. E. Huber, T. Best, S. S. Kumar, M. Probst and R. Wester, *J. Phys. Chem. A*, 2014, **118**, 6705–6710.
- 14 S. Trippel, J. Mikosch, R. Berhane, R. Otto, M. Weidemuller and R. Wester, *Phys. Rev. Lett.*, 2006, **97**, 193003.
- 15 P. Hlavenka, R. Otto, S. Trippel, J. Mikosch, M. Weidemuller and R. Wester, *J. Chem. Phys.*, 2009, **130**, 061105.
- 16 T. Best, R. Otto, S. Trippel, P. Hlavenka, A. v. Zastrow, S. Eisenbach, S. Jézouin, R. Wester, E. Vigren, M. Hamberg and W. D. Geppert, *Astrophys. J.*, 2011, **742**, 63.
- 17 S. S. Kumar, D. Hauser, R. Jindra, T. Best, Š. Roučka, W. D. Geppert, T. J. Millar and R. Wester, *Astrophys. J.*, 2013, **776**, 25.
- 18 J. E. Parr and J. L. Moruzzi, *J. Phys. D: Appl. Phys.*, 1972, **5**, 514.
- 19 Y. Okuyama, M. Sabo, H. Itoh and Š. Matejčík, *Eur. Phys. J.-Appl. Phys.*, 2013, **61**, 7.
- 20 M. Kučera, M. Stano, J. Wnorowska, W. Barszczewska, D. Loffhagen and Š. Matejčík, *Eur. Phys. J. D*, 2013, **67**, 1–8.
- 21 O. Martinez, Z. Yang, N. B. Betts, T. P. Snow and V. M. Bierbaum, *Astrophys. J.*, 2009, **705**, L172.
- 22 Z. Yang, C. A. Cole, J. Oscar Martinez, M. Y. Carpenter, T. P. Snow and V. M. Bierbaum, *Astrophys. J.*, 2011, **739**, 19.
- 23 R. Otto, J. Mikosch, S. Trippel, M. Weidemuller and R. Wester, *Phys. Rev. Lett.*, 2008, **101**, 063201.
- 24 M. Čížek, J. Horáček and W. Domcke, *J. Phys. B: At. Mol. Opt. Phys.*, 1998, **31**, 2571–2583.
- 25 T. González-Lezana, P. Honvault, P. G. Jambrina, F. J. Aoiz and J.-M. Launay, *J. Chem. Phys.*, 2009, **131**, 044315.
- 26 D. Gerlich and S. Schlemmer, *Planet. Space Sci.*, 2002, **50**, 1287–1297.
- 27 P. Jusko, Š. Roučka, R. Plašil and J. Glosík, *Int. J. Mass Spectrom.*, 2013, **352**, 19–28.
- 28 P. Jusko, Š. Roučka, D. Mulin, I. Zymak, R. Plašil, D. Gerlich, M. Čížek, K. Houfek and J. Glosík, *J. Chem. Phys.*, 2015, **142**, 014304.
- 29 J. C. Kleingeld and N. M. M. Nibbering, *Int. J. Mass Spectrom.*, 1983, **49**, 311–318.
- 30 T. M. Miller, A. A. Viggiano, A. E. S. Miller, R. A. Morris, M. Henchman, J. F. Paulson and J. M. V. Doren, *J. Chem. Phys.*, 1994, **100**, 5706–5714.
- 31 D. Hauser, O. Lakhmanskaya, S. Lee, Š. Roučka and R. Wester, *New J. Phys.*, 2015, submitted.
- 32 E. de Beer, E. H. Kim, D. M. Neumark, R. F. Gunion and W. C. Lineberger, *J. Phys. Chem.*, 1995, **99**, 13627–13636.

- 33 D. H. Zhang, M. Yang, M. A. Collins and S.-Y. Lee, *PNAS*, 2002, **99**, 11579–11582.
- 34 D. M. Neumark, *Phys. Chem. Chem. Phys.*, 2005, **7**, 433–442.
- 35 D. Wang, J. Z. H. Zhang and C.-h. Yu, *Chem. Phys. Lett.*, 1997, **273**, 171–178.
- 36 P. Jusko, O. Asvany, A.-C. Wallerstein, S. Brunken and S. Schlemmer, *Phys. Rev. Lett.*, 2014, **112**, 253005.
- 37 E. E. J. Muschlitz, *J. Appl. Phys.*, 1957, **28**, 1414–1418.
- 38 Y. Li, L. Liu and J. M. Farrar, *J. Phys. Chem. A*, 2005, **109**, 6392–6396.
- 39 J. J. Grabowski, C. H. DePuy and V. M. Bierbaum, *J. Am. Chem. Soc.*, 1983, **105**, 2565–2571.
- 40 A. A. Viggiano and R. A. Morris, *J. Chem. Phys.*, 1994, **100**, 2748–2753.
- 41 M. M.-N. Mautner, J. R. Lloyd, E. P. Hunter, W. A. Agosta and F. H. Field, *J. Am. Chem. Soc.*, 1980, **102**, 4672–4676.
- 42 S. T. Lee and J. M. Farrar, *J. Chem. Phys.*, 2000, **113**, 581–595.
- 43 M. Henchman and J. F. Paulson, *International Journal of Radiation Applications and Instrumentation. Part C. Radiation Physics and Chemistry*, 1988, **32**, 417–423.
- 44 J. R. Smith, J. B. Kim and W. C. Lineberger, *Phys. Rev. A*, 1997, **55**, 2036–2043.
- 45 P. A. Schulz, R. D. Mead, P. L. Jones and W. C. Lineberger, *J. Chem. Phys.*, 1982, **77**, 1153–1165.
- 46 K. K. Irikura, *J. Phys. Chem. Ref. Data*, 2007, **36**, 389–397.
- 47 K. Huber and G. Herzberg, *Molecular Spectra And Molecular Structure: Constants Of Diatomic Molecules*, Van Nostrand Reinhold, New York, 1979, vol. IV.
- 48 N. H. Rosenbaum, J. C. Owrutsky, L. M. Tack and R. J. Saykally, *J. Chem. Phys.*, 1986, **84**, 5308–5313.
- 49 L. I. Kleinman and M. Wolfsberg, *J. Chem. Phys.*, 1973, **59**, 2043–2053.
- 50 L. I. Kleinman and M. Wolfsberg, *J. Chem. Phys.*, 1974, **60**, 4740–4748.
- 51 A. Adohi-Krou, F. Martin, A. J. Ross, C. Linton and R. J. L. Roy, *J. Chem. Phys.*, 2004, **121**, 6309–6316.
- 52 B. Ruscic, A. F. Wagner, L. B. Harding, R. L. Asher, D. Feller, D. A. Dixon, K. A. Peterson, Y. Song, X. Qian, C.-Y. Ng, J. Liu, W. Chen and D. W. Schwenke, *J. Phys. Chem. A*, 2002, **106**, 2727–2747.
- 53 B. D. Rehfuss, M. W. Crofton and T. Oka, *J. Chem. Phys.*, 1986, **85**, 1785–1788.
- 54 D. Gerlich, G. Borodi, A. Luca, C. Mogo and M. A. Smith, *Z. Phys. Chem.*, 2011, **225**, 475–492.
- 55 G. Borodi, A. Luca and D. Gerlich, *Int. J. Mass Spectrom.*, 2009, **280**, 218–225.
- 56 I. Zymak, P. Jusko, Š. Roučka, R. Plašil, P. Rubovič, D. Gerlich and J. Glosík, *Eur. Phys. J. - Appl. Phys.*, 2011, **56**, 24010.
- 57 R. Plašil, I. Zymak, P. Jusko, D. Mulin, D. Gerlich and J. Glosík, *Phil. T. R. Soc. A*, 2012, **370**, 5066–5073.
- 58 D. Gerlich and S. Horning, *Chem. Rev.*, 1992, **92**, 1509–1539.
- 59 D. Gerlich, *Phys. Scripta*, 1995, **1995**, 256.
- 60 R. Wester, *J. Phys. B: At. Mol. Opt. Phys.*, 2009, **42**, 154001.
- 61 O. Asvany, S. Brunken, L. Kluge and S. Schlemmer, *Appl. Phys. B*, 2014, **114**, 203–211.
- 62 M. Hejduk, P. Dohnal, J. Varju, P. Rubovič, R. Plašil and J. Glosík, *Plasma Sources Sci. T.*, 2012, **21**, 024002.
- 63 I. Zymak, M. Hejduk, D. Mulin, R. Plašil, J. Glosík and D. Gerlich, *Astrophys. J.*, 2013, **768**, 86.
- 64 J. Glosík, D. Smith, P. Španl, W. Freysinger and W. Lindinger, *Int. J. Mass Spectrom.*, 1993, **129**, 131–143.
- 65 J. Glosík, W. Freysinger, A. Hansel, P. Spanel and W. Lindinger, *J. Chem. Phys.*, 1993, **98**, 6995–7003.
- 66 J. Glosík, P. Zakouřil and W. Lindinger, *Int. J. Mass Spectrom.*, 1995, **145**, 155–163.
- 67 J. Glosík, P. Zakouřil, V. Skalský and W. Lindinger, *Int. J. Mass Spectrom.*, 1995, **149-150**, 499–512.
- 68 J. Glosík, P. Zakouřil and W. Lindinger, *J. Chem. Phys.*, 1995, **103**, 6490–6497.
- 69 P. Zakouřil, J. Glosík, V. Skalský and W. Lindinger, *J. Phys. Chem.*, 1995, **99**, 15890–15898.
- 70 J. Glosík, P. Zakouřil and A. Luca, *Int. J. Mass Spectrom.*, 2003, **223-224**, 539–546.
- 71 D. R. Bates, *J. Phys. B: At. Mol. Phys.*, 1979, **12**, 4135.
- 72 E. Herbst, *J. Chem. Phys.*, 1979, **70**, 2201–2204.
- 73 M. Menzinger and R. Wolfgang, *Angew. Chem. Int. Ed. Engl.*, 1969, **8**, 438–444.